

Sl. No.	<p style="text-align: center;">IIT Ropar List of Recent Publications with Abstract Coverage: April, 2025</p>
A	<p style="text-align: center;">Book Chapter(s)</p>
1.	<p>Assessment of groundwater vulnerability of the Rupnagar block, Punjab, India using the DRASTIC-LUH model and electrical resistivity tomography T Prashanth, S Ganguly, D Banerjee, S Ganguly - Decontamination of Subsurface Water Resources System using Contemporary Technologies: Book Chapter, 2025</p> <p>Abstract: The groundwater in many places in our country is polluted due to the extensive use of fertilizers and pesticides in agriculture. These pollutants often infiltrate the ground surface and join the groundwater table, posing a significant risk to human health. Various thematic maps have been considered here to determine the areas prone to groundwater contamination, such as groundwater table depth, recharge rate, aquifer and soil characteristics, topography, vadose zone impact, and hydraulic conductivity. The groundwater vulnerability is determined by using the “entropy technique” and “technique for order of preference by similarity to ideal solution” (TOPSIS) method. The study found that 25.10% of the Rupnagar block has a high potential for groundwater contamination from intensive agricultural activities. At highly vulnerable zones, it is observed that the longitudinal conductance obtained by using electrical resistivity tomography (ERT) is less than 0.1 mho, which signifies less aquifer protective capacity.</p>
B	<p style="text-align: center;">Conference Proceeding(s)</p>
2.	<p>Advancing oilfield intelligence: Exploring machine learning operations in volve MM Laljee, AH Sahir - Proceedings of 1st International Conference on Petroleum, Hydrogen and Decarbonization (ICPHD 2023), 2025</p> <p>Abstract: Traditionally, analytical and numerical methods have been used to model oil and gas exploration and production (E&P) activities. However, these methods have their own disadvantages to which machine learning (ML) provides a solution. With the help of ML, data-driven models can be created using limited data to gain quality insights. In this study, chiefly two ML algorithms have been used- random forest regression and long short-term memory (LSTM) to create an end-to-end workflow which assists crucial E&P activities. The study is based on open-source data from the Volve oilfield released by Equinor. Continuous learning models have been developed for rate of penetration prediction in well drilling and oil and gas production forecasting, where both subsurface and over-ground parameters influence the results. On the other hand, a sonic log prediction model is created using reference wells and validated using blind data, where the results are influenced by subsurface parameters only. These models perform satisfactorily, with the R^2 ranging from 0.54 to 0.85. Despite the apparently low R^2 values, the models do a pretty good job in capturing the information and insights that can be gleaned from the data.</p>
3.	<p>Design and analysis of optimized mast structure for a blade-less wind turbine KK Verma, S Sonkar, P Majhi, Vishal, AVR Teja - IECON 2024 - 50th Annual Conference of the IEEE Industrial Electronics Society, 2025</p> <p>Abstract: Mast is the foundation body in a bladeless wind turbine, its interaction with fluid (air or water) generates vibrations that in turn harvest usable electricity. Care must be taken while designing the structure of mast, in order to have an efficient generation of electricity. Having an optimum design of mast not only increases efficiency but also ensures the stability and longevity</p>

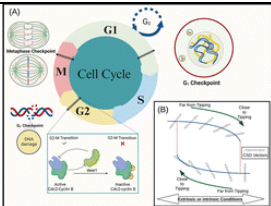
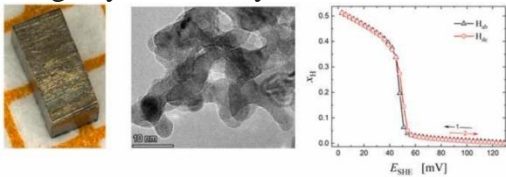
	<p>of the entire bladeless wind turbine system. This article focuses on the design and analysis of various mast on a number of various parameters in order to obtain an optimum design and structure of the mast. The design was analysed using "Ansys® Mechanical" 2020R2, the results and comparison has been provided in this article.</p>
4.	<p>Development of a precise regional-scale groundwater model by coupling MODFLOW & Machine Learning algorithms: A case study in Bist-Doab region, Punjab, India A Kantode, T Prashanth, S Ganguly - EGU General Assembly, 2025</p> <p>Abstract: Groundwater depletion in the Bist-Doab region of the Punjab State of India is a significant threat to sustainable agricultural practices, underscoring the need for effective management strategies. Modelling groundwater heads is essential for understanding groundwater flow dynamics, trends, and their interaction with surface water. It helps assess the aquifer's health, prevent over-extraction and contamination, and predict ambient groundwater responses to extreme events such as droughts or floods. Inaccurate groundwater models, which overestimate or underestimate groundwater levels and fail to capture temporal fluctuations, hinder proper water management. These errors lead to suboptimal decisions regarding water allocation and resource sustainability and ultimately impact crop yields and water availability. This study aims to integrate physically-based models, such as those developed by MODFLOW, with machine-learning algorithms to improve prediction accuracy and support more informed decision-making. MODFLOW was used to simulate groundwater flow under both steady-state and transient conditions, utilizing field hydrogeological data from existing literature. Machine learning (ML) models, including Support Vector Regression (SVR), Random Forest (RF), and Artificial Neural Networks (ANN), were trained and tested on historical groundwater levels and meteorological data to enhance prediction accuracy. The methodology employs data-driven models (DDMs) as error-correcting tools for the physically-based models. Historical residuals, calculated as the difference between observed and simulated groundwater heads, were used as inputs alongside features such as well location coordinates, simulated groundwater heads, and time of measurements. ML techniques such as SVR, RF and ANN were used to train the DDMs, which learn systematic errors in the physically-based model by analysing these historical residuals. Outputs include predicted systematic errors and updated groundwater heads, where corrections are applied to the initial simulated values. The effectiveness of the DDMs relies on the structure and patterns of the residuals in the physically-based model, with strong correlations between the groundwater heads, leading to better error correction and improved predictive accuracy. Results show that integrating MODFLOW with ML, significantly reduces model error compared to traditional simulation approaches. The combined model effectively captures both seasonal fluctuations and long-term trends in groundwater levels, leading to more accurate predictions. The developed framework provides a reliable tool for improving groundwater resource management and optimizing water allocation strategies, ultimately supporting the sustainable management of groundwater in agriculturally stressed regions like Bist-Doab.</p>
5.	<p>GPU accelerated construction of time respecting data structure for temporal graphs A Naskar, VK Tavva, S Banerjee - 2024 IEEE High Performance Extreme Computing Conference (HPEC), 2025</p> <p>Abstract: The transformation of a temporal graph into its corresponding time-respecting graph (TRG) offers significant advantages for neighborhood search problems when compared to the traditional edge stream representations. However, constructing TRGs is a time-consuming process that can be substantially accelerated using GPU based parallelism. In this paper, we propose a novel highly parallel method to construct the timerespecting graph (TRG) from the edge list by leveraging GPU parallelism. For graphs of various sizes, ranging from 0.05 to 33 million edges, we achieve a speedup of up to 387x over the sequential variant on comparable hardware. We demonstrate that our method produces TRG in the standard CSR form that can be input to high-performance graph analytics libraries such as nvGRAPH. The TRG produced is</p>

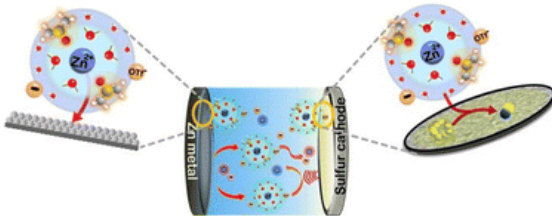
	also optimized for a minimal number of vertices and edges. Our method also provides support for efficient real-time dynamic updates to the temporal graph.
6.	<p>Impact of discretization techniques on model predictive control of SRMs P Prabhat, AVR Teja - IECON 2024 - 50th Annual Conference of the IEEE Industrial Electronics Society, 2025</p> <p>Abstract: Model Predictive Control (MPC) techniques provide high performance and reduced torque ripple in switched reluctance motor (SRM) drives. However, the accuracy of MPC is sensitive to the accuracy of the prediction obtained using discretization of the SRM model. Most of the literature uses only the forward-euler discretization technique in the MPC of SRM drives. However, the performance of other available discretization techniques remains unknown. Therefore, in this paper, three different discretization techniques (Forward euler, Heun,s method and Runge-Kutta (IInd and IVth order methods) are analyzed for the implementation of model predictive control on SRM drives, and their performances are compared. All the techniques have been implemented on an 8/6 4-phase SRM drive using MATLAB/Simulink, and the results are presented.</p>
7.	<p>PULSE: Physiological understanding with liquid signal extraction S Ahmad, S Bano, S Verma, YS Rawat, S Chanda, SK Vipparthi, S Murala - 2025 IEEE/CVF Winter Conference on Applications of Computer Vision (WACV), 2025</p> <p>Abstract: The non-contact estimation of vital signs, particularly heart rate, from video data is a promising method for remote health monitoring. 3D convolutional layers are widely used for this task due to their ability to capture both spatial and temporal features. However, traditional 3D convolutions, while effective in many cases, lack the capacity to adjust dy-namically to the temporal variability inherent in physiological signals such as remote photoplethysmography (rPPG), which are characterized by subtle frequency changes over time. To address this, we propose PULSE (Physiological Understanding with Liquid Signal Extraction), a frame-work that employs Liquid Time-Constant (LTC) models with 3D convolutional layers to enhance temporal sensitivity and improve the extraction of these fine-grained rPPG signals. In PULSE, traditional 3D-conv layers are deployed for ini-tial feature extraction, while LTC-based 3D-conv layers dy-namically adapt and guide the temporal processing, allowing the model to better track and interpret the subtle variations in heart rate signals under different conditions, such as motion artifacts and lighting changes. We evaluated the effectiveness of PULSE in an unsupervised training setting, demonstrating that our solution performs well even in the absence of labeled datasets a common challenge in rPPG signal extraction. Experimental evaluations on three public datasets confirm that PULSE achieves comparable or supe-rior results to existing methods, proving its robustness and efficacy for real-world, non-contact health monitoring applications.</p>
8.	<p>Strategic high-frequency switching of idle phases for static & dynamic eccentricity detection in switched reluctance motors M Alam, S Payami - IECON 2024 - 50th Annual Conference of the IEEE Industrial Electronics Society, 2025</p> <p>Abstract: Switched reluctance motors (SRMs) inherently exhibit issues such as torque ripples, noise, and vibrations, which are exacerbated by eccentricities. Eccentricity, one of the most common mechanical faults in SRMs, worsens with continued operation due to unbalanced magnetic pull. In extreme cases, this can lead to physical contact between the stator and rotor poles, causing irreversible damage to the motor. This article presents a scheme for the online diagnosis of static eccentricity (SE) and dynamic eccentricity (DE) in SRMs by switching the phases at a higher frequency in their respective negative torque regions. This technique leverages variations in inductance profiles caused by eccentricities to identify and distinguish between SE and DE, and to detect the phase along with which the rotor pole has shifted in case of SE. The proposed scheme has been validated through finite element method-based simulations in an</p>

	ANSYS Maxwell environment for a 4-phase 8/6 SRM.
9.	<p>Structural alteration and electric field estimation inside HVAC cable due to inhomogeneous aging P Sharma, PK Pandey, CC Reddy - 2024 IEEE Conference on Electrical Insulation and Dielectric Phenomena (CEIDP), 2025</p> <p>Abstract: Under diverse loading conditions, high-voltage alternating current (HV-AC) underground polymeric cables exhibit a radial temperature gradient and experience differential thermal stress, resulting in inhomogeneous aging of the polymeric material. Consequently, a differential localized structural alterations occur at different radial positions within the insulation bulk of the cable. To investigate these effects, the authors have examined the cross-linked polyethylene (XLPE) insulation taken from HV-AC cables. Using a lathe machine, samples were extracted and subjected to various tests. The findings revealed significant variations in the morphology of the XLPE layers at different radial positions within the cable insulation bulk. These effects were further investigated by measuring the permittivity of samples extracted from different radial positions within the insulation bulk. The permittivity data is then fitted to field, temperature and radial position dependent equation, and the AC electric field distribution is estimated. The findings are also corroborated by AC breakdown tests.</p>
10.	<p>Supervised NN model for data augmentation of 4D PES and application in quantum dynamics A Kushwaha, TJ Dhillip Kumar - 2024 IEEE 31st International Conference on High Performance Computing, Data, and Analytics Workshops (HiPCW), 2025</p> <p>Abstract: The study aims to utilize neural network (NN) models for augmenting molecular potential energy surfaces (PES) within spectroscopic accuracy (i.e. error $< 1 \text{ cm}^{-1}$). The current methods for solving the Schrödinger equation within such accuracy scale poorly with system size. The PES is an essential starting point for studying any quantum dynamical process occurring in a given molecular system. Since the molecular Hamiltonian quickly surpasses the current computing limits due to the large dimensionality of the equation, the scalability and ability to handle a large number of dimensions make NN models an ideal candidate for such applications. The current paper takes an example of an NCCN-H2 collisional system which results in a 4D PES under rigid rotor approximation. Several supervised NN models are created and benchmarked by splitting the dataset into training and testing datasets. The final model can augment the PES within hours, delivering results that otherwise need years of computation.</p>
11.	<p>Targeted output driven dataset generation methodology for training neural network controllers in specific n^{th} order systems AH Kumar, AVR Teja - IECON 2024 - 50th Annual Conference of the IEEE Industrial Electronics Society, 2025</p> <p>Abstract: The performance of a neural network controller majorly depends on the dataset used for training. Traditionally, Proportional-Integral (PI) controller data is used to train a neural network. In this scenario, the performance of the neural controller is limited by the performance of the PI. Similarly, any other controller data, when used, restricts the neural controller's performance within its limitations. In this paper, a targeted output-driven dataset that theoretically gives the best desirable response is derived and used for training the neural controllers. Therefore, enhanced performance could be achieved that is better than that of traditional PI controllers. Detailed theoretical derivations are provided for obtaining the proposed dataset generation methodology for any n^{th} order system without zeros. The viability of the proposed neural controller was simulated and trained in a MATLAB/Simulink environment, and its response to variation in reference input has been inferred. The performance comparisons are made with the PI controller data and presented.</p>
12.	<p>TRUST: Time-domain residual unsupervised stability technique for improved heart rate estimation</p>

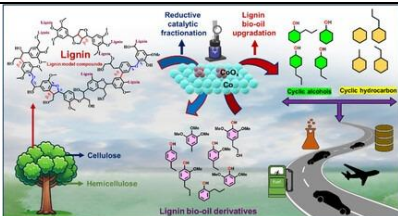
	<p>S Ahmad, S Bano, S Chanda, SK Vipparthi, S Murala - 2025 IEEE/CVF Winter Conference on Applications of Computer Vision (WACV), 2025</p> <p>Abstract: Camera-based estimation of vital signs is a promising method for non-contact health monitoring, which analyzes minute changes in video data. However, the creation of accurate models for this task is challenging due to the scarcity of datasets that possess synchronized vital sign recordings. Our research enhances an existing non-contrastive unsupervised learning technique for extracting rPPG signals, which does not necessitate ground-truth signals during the training process. We have incorporated new time-domain loss functions and added a feature stabilization block to improve the model's stability and accuracy in detecting low-level features. Additionally, we have devised a metric to evaluate the feature instability in the model's final layer. Our experiments on four public datasets demonstrate that our method surpasses the performance of current state-of-the-art methods. These advancements make our approach a significant breakthrough in the development of scalable deep-learning models for camera-based heart-rate estimation.</p>
13.	<p>Two-stage, global-local approach for cell nuclei segmentation in histopathology images A Shakya...S Naidu, S Murala... - 2024 IEEE 8th International Conference on Information and Communication Technology (CICT), 2025</p> <p>Abstract: Effective management of high-resolution, and spatially wide contextual cues is fundamental to the accurate semantic segmentation. Traditional approaches like multi-resolution feature maps, and skip-connection are effective but require changes in the backbone architecture, restricting utilization of newer models and architectures for the problem. In this work we propose an architecture-agnostic, two-stage, global-local frame-work, called GoLo, for the semantic segmentation, which can use arbitrary semantic segmentation models within its two stages. We focus on segmenting cell nuclei in histopathology image analysis, where accurate segmentation of cell nuclei boundaries is one of the key issues. The proposed framework consists of first stage with Global and second stage with Local learning approach. The first stage is proposed to process the image globally and provide the coarse nuclei segmentation map. In the second stage, to process the image locally, coarse segmentation map and input image is first converted into patches. These patches are then fed as input to the second stage to get the fine- grained segmentation map. Both stages are trained with a combination of dice and binary cross entropy loss. To show the effectiveness of our approach, we test 4 state-of-the-art segmentation architectures (ACC-UNet, UCTransnet, Swin-UNet, and Vanilla U-Net), on 4 different benchmark datasets (MoNuSeg, CPM-17, CoNSep, and TNBC). We evaluate performance of each technique before and after using our framework. We report an average improvement of 4.82 % in mIoU, and 4.52% mDSC score, across techniques, and datasets.</p>
14.	<p>USWformer: Efficient sparse wavelet transformer for underwater image enhancement P Mishra, N Mehta, SK Vipparthi, S Murala - 2025 IEEE/CVF Winter Conference on Applications of Computer Vision (WACV), 2025</p> <p>Abstract: Transformer-based methods have shown great promise in underwater image enhancement (UIE) tasks due to their capability to model long-range dependencies, which are vital for reconstructing clear images. While numerous effective attention mechanisms have been devised to handle the computational requirements of transformers, they frequently incorporate redundant information and noisy interactions from irrelevant regions. Additionally, the current methods focusing solely on the raw pixel space constrains the exploration of the underwater image frequency dynamics, thus hindering the models from fully leveraging their potential for producing high-quality images. To address these challenges, we propose USWformer, an efficient UIE Sparse Wavelet Transformer Network (1.19 M parameters) to eliminate the redundant features in both the spatial and frequency domains. The USWformer consists of two fundamental components: a Sparse Wavelet Self-Attention (SWSA) block and a Multi-scale</p>

	Wavelet Feed-Forward Network (MWFN). The SWSA block selectively preserves essential attention scores from the keys corresponding to each query, adjusting the feature details. MWFN further diminishes the feature redundancy in the aggregated features thereby improving the enhancement of the underwater images. We assess the efficacy of our approach across benchmark datasets comprising synthetic and real-world under-water images, showcasing its superiority via thorough ablation studies and comparative analyses.
C	Journal Article(s)
15.	<p>A critical assessment of electrical conductivity and multifunctionality of MWCNT/Epoxy nanocomposites H Gupta, M Srivastava, PK Agnihotri... - IEEE Transactions on Dielectrics and Electrical Insulation, 2025</p> <p>Abstract: Using available data from the literature and our own results, we critically examine the multi-functionality of epoxy-multiwalled carbon nanotube (MWCNT) composites. A major advantage of adding MWCNT is that the key properties of the pristine epoxy are largely retained or even bettered. The manner in which the synthesis process affects the dispersion of the nano-fillers and their properties is studied. Ideas from percolation theory are used to study and understand the nature of the variation of DC electrical conductivity with filler content, and that of AC conductivity with both filler content and frequency. The electromagnetic shielding effectiveness over a broad microwave frequency range is investigated. Tensile strength, fracture properties and thermal conductivity of the nanocomposites are also investigated. Thus the multi functionality of MWCNT-epoxy composites is critically assessed. Overall, we demonstrate that a deep understanding of the conduction mechanisms has been achieved. Also, the limitations of these materials have been identified and potential applications are mapped out. Their use as tough and durable electrically conductive adhesives is indicated. It is also shown that the major impediments to more versatile applications of these materials are their poor thermal conductivity and loss of flowability with increasing MWCNT content.</p>
16.	<p>A general, robust framework for determining the key species that forewarns sudden transitions in biological circuits D Kashyap, T Kaur, P Dutta, S Sinha - Physical Chemistry Chemical Physics, 2025</p> <p>Abstract: The Cdc2-cyclin B/Wee1 kinase system exhibits bistability between alternative steady states, which emerges due to the mutual inhibition between Cdc2-cyclin B and Wee1 kinases. Alternative steady states are the M phase-like state and G2 arrest state, which have implications in cell cycle progression at the G2 phase in eukaryotic cells. A slight alteration in the feedback strength can drive sudden transitions between these contrasting alternative states upon crossing a critical threshold or a tipping point. The phenomenon of critical slowing down (CSD) has been widely used to identify the proximity to a tipping point. However, determining the key variable or species that best signals CSD is a challenging task and holds significance in complex biochemical processes. Here, we determine the key variable or observation direction (OD) from the direction of CSD to best detect an upcoming transition in the Cdc2-cyclin B/Wee1 model system. We find that with increasing feedback strength, the Cdc2-cyclin B is the OD, as it produces a stronger signal than that of Wee1. With decreasing feedback strength, both Cdc2-cyclin B and Wee1 produce similar signals and can be used as the OD. Furthermore, the noise-sensitive direction highlights the effect of stochasticity in Cdc2-cyclin B and Wee1 for increasing and decreasing feedback strength, respectively. We also perform sensitivity analyses that reveal the robustness of the OD. Finally, we compare the efficacy of OD with principal component analysis while detecting a tipping point, and also validate its general applicability to epithelial–mesenchymal transition for cancer progression.</p>

		
17.	<p>A new and unified semi-analytical method with a convergence acceleration parameter for linear and nonlinear fragmentation equations S Keshav, M Singh...J Kumar - Proceedings of the Royal Society A: Mathematical, Physical and Engineering Sciences, 2025</p> <p>Abstract: In recent years, turbulent multiphase flows, including bubbles and droplet breakup, have been commonly modelled using linear fragmentation population balance equations (PBEs) to capture droplet distribution effectively. These models often rely on binary breakup kernels, where two particles form due to external forces, while particle–particle collisions are neglected to simplify the physics. The mathematical complexities of collisional breakage models stem from the intricate structures of the collisional and fragmentation kernels, along with nonlinear integrals, which limit their applicability in real-world scenarios. These complex kernel structures also constrain the availability of analytical solutions for simple collisional and fragmentation kernels. To address this, a unified approximation method with a convergence acceleration parameter is proposed for both linear and nonlinear fragmentation problems. By optimizing the acceleration parameter, the method extends the convergence zone of series solutions over longer time domains and resolves issues present in existing approaches. A detailed theoretical convergence analysis of the proposed method in Banach space is provided. Various analytically tractable and physically relevant kernels, with different initial conditions (ICs) such as Dirac delta, exponential, gamma and Gaussian distributions, are used to validate the accuracy of this approach against the homotopy perturbation method and BLUES function method.</p>	
18.	<p>A Pd-Pt-based bulk nanoporous alloy with continuous solubility for hydrogen S Bapari, J Weissmüller - Electrochimica Acta, 2025</p> <p>Abstract: Metal hydrides that enable reversible solute exchange with a reservoir often exhibit a miscibility gap at room temperature. Misfit strain during two-phase coexistence may then lead to degradation on repeated charging/discharging cycles. Furthermore, the miscibility gap impairs continuous and uniform composition tuning for functional applications. We explore electrochemical dealloying as a pathway to macroscopic monolithic samples of nanoporous Pd–Pt with continuous solubility for H at room temperature. The ligament size is tunable in the range of 4–40 nm, and sorption isotherms suggest a miscibility-gap critical point marginally below room temperature. With a maximum hydrogen fraction of 0.5, we demonstrate a reversible actuation strain of 3.3 % and a high cycle stability.</p> 	
19.	<p>Achieving high capacity and long cycling life in aqueous zinc-sulfur batteries with improved kinetics through electrolyte solvation engineering TS Thomas, AP Sinha, D Mandal - EES Batteries, 2025</p> <p>Abstract: Aqueous Zn/S batteries are emerging as promising next-generation high-energy density rechargeable storage devices. The cost-effective and abundant reserve of sulfur, when paired with a zinc anode, significantly enhances both specific capacity and energy density. However, their practical applications face challenges such as poor sulfur utilization in aqueous</p>	

	<p>electrolytes, sluggish sulfur redox kinetics and parasitic reactions at the Zn anode. To address these challenges, electrolyte engineering strategies have been introduced using high donor number (DN) organic co-solvents. Extensive investigation into the impact of DN on sulfur conversion kinetics and the Zn anode reveals that DMSO, a high-DN solvent, facilitates efficient reversibility of sulfur and prevents the hydrogen evolution reaction (HER) and dendrite formation on the zinc anode by modulating the solvation sheath of Zn^{2+} ions. Notably, the high DN of DMSO enables a lower concentration of additives while improving the kinetics of both the sulfur cathode and the zinc anode, compared to higher concentrations of low-DN solvents like acetonitrile and DMF. As a result, the Zn/S battery with a DMSO-containing electrolyte achieved a high specific capacity of 1502 mA h g^{-1} at 0.1 A g^{-1} and long-term cycling stability with 92% capacity retention over 1000 cycles at 5 A g^{-1}.</p> 
20.	<p>Adaptive ML MISO receiver: Conditional fine-tuning without CSI A Ahmad, S Agarwal - IEEE Transactions on Green Communications and Networking, 2025</p> <p>Abstract: This paper introduces a novel machine learning-based receiver for symbol detection in a Multiple-Input Single-Output system, optimized for next-generation vehicular networks. The receiver operates without channel state information (CSI), leveraging an innovative feature selection strategy that enhances its adaptability to dynamic, real-world communication environments. Key components include Neural Adaptive Symbol Detection (NASD), which provides an initial detection framework, and the Context-Enhanced Symbol Detector (CESD), a fine-tuning mechanism that dynamically adjusts to varying signal conditions. These innovations equip the receiver with robustness against unpredictable vehicular communication challenges, such as rapid movement, Doppler effects, and multipath fading. The system is evaluated using testbed featuring a custom-built UAV to emulate complex vehicle dynamics. This setup enables rigorous testing under a variety of conditions, including static, maneuvering, and hovering scenarios. Experimental results demonstrate the receiver's ability to sustain low bit error rates across a wide range of signal-to-noise ratios, significantly outperforming non-adaptive methods, especially in dynamic environments. The combination of NASD and CESD facilitates real-time adaptation without the need for CSI or extensive pre-training, establishing this approach as an efficient, low-complexity receiver solution for modern vehicular communication systems.</p>
21.	<p>Assessment of the effects of core decompression on the patho-biomechanics of the femoral head in avascular necrosis: A biomechanical perspective AM Kurup, RK Bhushan, N Kumar, N Kumar, RK Sen - Injury, 2025</p> <p>Abstract: Background: Avascular necrosis (AVN) of the femur head (FH) is an incapacitating disease caused by chronic overconsumption of alcohol and corticosteroids. AVN impairs blood circulation to the FH, causing varying degrees of cell death. AVN progressively reduces the macroscopic mechanical strength of the bone's necrotic area, leading to FH collapse. Material and method: This study aims to comprehend the efficacy of core decompression (CD) on biomechanical, microstructural, and compositional determinants of bone quality. In this work, 30 FH are taken of the patients who underwent total hip replacement due to AVN. These 30 samples are categorized into two groups (15 each), i.e. with CD (individuals who underwent core decompression treatment at the early stages of AVN) or without CD (individuals who did not receive any invasive therapy in the past following a hip fracture due to AVN). Bone morphometry, biomechanical, material, and nano-level properties are analyzed across necrotic</p>

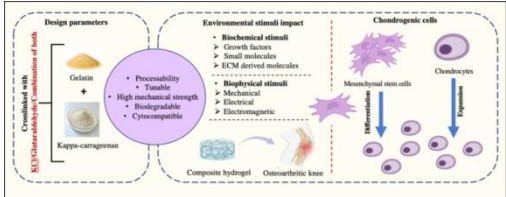
	<p>and sclerotic zones of FH through micro-CT scanning, histo-pathology, Uni-axial compression, and Nano-indentation tests. Results: The obtained results demonstrated a notable increment in bone volume fraction, ultimate strength, and osteocytes of the sclerotic zone of both groups compared to the necrotic region. A significant improvement was observed in the quality of trabecular bone at multiple scales of human bone tissue including higher bone volume fraction (22.87 %, $P < 0.05$), increased Young's modulus (28.80 %, $P = 0.0183$) and increment in Mineral/Matrix ratio (53.20 %, $P = 0.0429$) and reduction in % of empty lacunae (22.39 %, $P < 0.01$) in the necrotic region of patients with core decompression compared to patients without any invasive treatment. Conclusion: The optimum core decompression enhances the stability of the femur head by increasing the macroscopic mechanical strength of necrotic bone and decreasing the strength of sclerotic bone. This brings the strength of both bones nearly equal, further reducing the stress gradient and probability of collapse of the AVN femur head.</p>
22.	<p>Boosted electrochemical CO₂ reduction via hydrogen sulfide oxidation driven proton diffusion S Kaur, K Garg, M Kumar, TC Nagaiah - Advanced Functional Materials, 2025</p> <p>Abstract: Natural gas sweetening is irrefutable in mitigating the detrimental impacts of hazardous and corrosive pollutants like carbon dioxide (CO₂) and hydrogen sulfide (H₂S) on industries and the environment. Consequently, simultaneous conversion of CO₂ and H₂S into value-added products is of great demand, alternative to expensive and energy consuming methods. Herein, a bifunctional electrocatalyst (NiCo(<i>x</i>:<i>y</i>)S_n) utilized for CO₂ reduction reaction (CO₂RR) and H₂S oxidation in a tandem electrolytic cell exhibited remarkable activity toward CO₂ to methanol and ethanol with a Faradaic efficiency (F.E.) of 29.26% and 50.16%, respectively, and H₂S electrolysis (sulfide oxidation reaction, SOR) to sulfur with 79.9% yield. Besides, co-electrolysis <i>viz.</i>, anodic H₂S oxidation strategy to facilitate the cathodic CO₂RR with reduced energy consumption and to achieve value-added products at both electrodes offers “<i>one stone-two birds</i>” strategy: a pollutant remediation along with the production of value added products. Notably, a cell voltage of 0.785 V is saved by CO₂RR-SOR compared to conventional CO₂RR-OER cells with enhanced yield rates. The plausible mechanistic pathway for CO₂RR and its enhanced electrocatalytic activity due to H₂S oxidation by proton diffusion strategy is probed via in situ electrochemical Fourier transform infrared spectroscopy (FT-IR) which is further supported by four probe electrochemical approach.</p>
23.	<p>Catalytic hydrogenation of lignin ethers and bio-oil using non-noble cobalt catalysts BP Singh, A Kumar, R Bal, R Srivastava – ChemSusChem, 2025</p> <p>Abstract: The conversion of lignocellulosic biomass into lignin bio-oil and its subsequent upgrading into saturated cyclic products holds considerable promise for applications in the aviation industry. This study reports the synthesis of a defect-enriched monometallic CoO_x/Co-350-30 catalyst, which is utilized for hydrogenating lignin-derived molecules and lignin bio-oil obtained via reductive catalytic fractionation (RCF) of wheat straw. Under optimized conditions (180 °C, 2 MPa H₂, 2 h), benzyl phenyl ether (BPE) affords complete conversion, yielding ≈99% cyclohexanol and ≈98% methylcyclohexane. RCF of wheat straw (conducted at 230 °C and 3 MPa H₂ for 6 h) affords lignin bio-oil containing ≈43% alkyl-substituted phenols. Hydrogenation of the bio-oil using the CoO_x/Co-350-30 catalyst (at 250 °C for 2 h at 3 MPa H₂) results in ≈98% yield of cyclic aliphatic alcohols. Comparative studies with commercial 5%Ru/C reveal that the CoO_x/Co-350-30 catalyst produced products with lower oxygen functionalities and fewer native lignin linkages. Comprehensive catalyst characterizations and activity tests were conducted to propose a plausible reaction mechanism for BPE hydrogenation. The cobalt-based catalyst, devoid of noble metals, provides a sustainable and cost-effective method for biomass conversion into fuel-range products, addressing the growing industry demand for more efficient catalytic processes.</p>

		
24.	<p>Collective excitations and universal coarsening dynamics of a spin-orbit-coupled spin-1 Bose-Einstein condensate Rajat, P Banger, S Gautam - Physical Review A, 2025</p> <p>Abstract: We study the collective excitation spectrum of a Raman-induced spin-orbit-coupled spin-1 Bose-Einstein condensate confined in a quasi-one-dimensional harmonic trap while varying either the Raman coupling or quadratic Zeeman field strength by using the Bogoliubov approach. A few low-lying modes, which can be used to delineate the phase boundaries, are identified by exciting them with suitable perturbations. We also investigate the coarsening dynamics of a homogeneous quasi-two-dimensional spin-orbit-coupled spin-1 condensate by quenching from the zero momentum into the plane wave phase through a sudden change in Raman coupling or quadratic Zeeman field strength. We demonstrate that the correlation function of the order parameter displays dynamic scaling during the late-time dynamics, allowing us to determine the dynamic critical exponent.</p>	
25.	<p>Collisional dynamics of newly detected protonated dicyanoacetylene (NC_4NH^+) with heat low interstellar temperatures P Chahal, TJ Dhilip Kumar - Journal of Computational Chemistry, 2025</p> <p>Abstract: Cyanopolyynes and protonated-dicyanopolyynes molecules always get special attention for their detection in the interstellar medium. The rotational quantum dynamics for the collision of recently detected protonated dicyanoacetylene (NC_4NH^+) with He is studied to get the inelastic rate coefficients till temperature range of 100 K. An accurate potential energy surface (PES), computed using ab initio methods, has been developed for the $\text{NC}_4\text{NH}^+ - \text{He}$ collision system. The PES was developed with the coupled cluster, that is, the CCSD(T)-F12b method in combination with the aug-cc-pVTZ basis set. The 2D PES has a global minimum with a value of -239.19 cm^{-1}. The analytical fitting of this 2D PES is done to obtain the radial coefficients, that give cross-sections for NC_4NH^+ molecule till collisional energy range of 300 cm^{-1}. The rate coefficients are achieved for the first 20 rotational transitions. An important trend is observed when comparing the de-excitation rate coefficients at different temperatures. For transitions below $\Delta j = 10$, a preference for odd Δj values is evident, which can be attributed to the anisotropy in the PES of the $\text{NC}_4\text{NH}^+ - \text{He}$ collision. This similar behavior is observed for $\text{HC}_3\text{NH}^+ - \text{He}$ collision. However, for higher transitions, a strong propensity for even Δj transitions emerges. The results obtained in the present work will enable us to estimate the abundance of NC_4NH^+ in the ISM under non-local thermal equilibrium conditions.</p>	
26.	<p>Comparative analysis of electrostatic filtration in pilot pulse-jet and flat-based test rigs S Dutta, A Mukhopadhyay...CC Reddy - Indian Journal of Fibre & Textile Research (IJFTR), 2025</p> <p>Abstract: This study investigates the filtration performance of three different filter media—PTFE (Polytetrafluoroethylene)-coated media, stainless steel fibre blended with PET (Polyethylene Terephthalate) media, and stainless steel fibre scrim media—under varying charge levels and dust concentrations using a pilot pulse-jet filter unit and a flat-based test rig. The effect of charge, material type, and dust concentration on filtration efficiency, particulate emissions, and charge dissipation behaviour is systematically examined. Results indicate that charge plays a dominant role in enhancing filtration efficiency by promoting dust agglomeration and improving</p>	

	<p>dust cake properties. PTFE-coated media exhibits the lowest particulate emissions across both test rigs, whereas stainless steel fibre scrim media demonstrates the fastest charge dissipation. A comparative analysis reveals that the pilot pulse-jet filter unit exhibits higher particulate emissions than the flat-based test rig due to its non-uniform dust deposition and cleaning inefficiencies. The study further establishes strong correlations between downstream particulate emissions, mass concentration, and particle number concentration across the two test rigs. Findings provide valuable insights into optimising charge-assisted filtration mechanisms and understanding the influence of electrostatic charge on different filter media.</p>
27.	<p>Comparative life cycle assessment of conductive polyester filters on flat and pilot filtration test rigs under varying aerosol pre-charge S Dutta, A Mukhopadhyay...CC Reddy - Journal of The Institution of Engineers (India): Series E, 2025</p> <p>Abstract: The life cycle of the filter material is an important factor to take into account when evaluating the commercial benefit for any gaseous filtration company. For a filter media to last as long as possible, it should consistently provide filtrate for a long time. Because of this, the current work aims to anticipate the ageing behavior of three distinct polyester conductive filter materials through experimental characterization: TEFLON coated media, Carbon Fibre Blended with PET, and Carbon Fibre Scrim Media. Using fly ash aerosol, the materials were tested on two distinct laboratory-based test rigs, namely the flat-based and pilot-filter unit, at two different dust densities (50 g/m^3 and 90 g/m^3). Three degrees of pre-charging were applied to the aerosol via a coaxial cable viz. 2 kV, 5 kV and 9 kV. The results showed that, for all materials, both test rigs performed better at aging at higher levels of aerosol charge. Under all operational conditions, however, it has been discovered that the flat media test rig performs better relative to the other options. Because of its improved surface qualities as a result of coating, TEFLON coated materials have been determined to have the best ageing behavior among all the materials studied in both test rigs.</p>
28.	<p>Comparison of Q parameter in stationary and growing creep cracks in SS316LN with 0.07% nitrogen at 650 oC AK Mishra, R Upadhyaya...A Tiwari - Theoretical and Applied Fracture Mechanics, 2025</p> <p>Abstract: This study explores the influence of in-plane constraint on the creep crack behavior of a new variant of SS316LN with 0.07% nitrogen under stationary and growing cracks through experimental and numerical approaches. The Q parameter is calculated to characterize the in-plane constraint, while the C* parameter is used to analyze creep deformation and fracture behavior. Comprehensive experimental tests and finite element simulations provide insights into the interaction between in-plane constraints and crack-tip stress fields. The results enhance the understanding of constraint effects in stationary crack scenarios, contributing to the development of improved methodologies for high-temperature failure assessments and life prediction of structural components made of SS316LN.</p>
29.	<p>Controlled harnessing of azobenzene photoswitches in neat states through modulated self-assembled mesogenic nanostructures A Krishna KM, Ashy, M Gupta - Advanced Sustainable Systems, 2025</p> <p>Abstract: This study introduces visible-light responsive self-assembled liquid crystals (LC) by the innovative integration of a tetra-<i>ortho</i>-substituted azobenzene dopant into imidazolium-based ionic liquid crystalline (ILC) host matrix. Comprehensive analyses using differential scanning calorimetry, polarized optical microscopy, and wide-angle X-ray scattering confirm the formation of various stable mesophases based on the amount of dopant. By synergistically combining the photoresponsiveness of azobenzene with the LC order of the ILC host, materials capable of efficient photothermal energy conversion in solid-states are engineered. This strategic</p>

	<p>fusion of components is designed to create a dynamic system with rapid photoswitching capabilities and substantial energy storage density. By meticulously modulating the concentration of azobenzene within the ILC matrix, materials with remarkable half-lives and charging capacity of up to 78% in thin films are engineered. The heat release dynamics, observed for films charged under green LED, revealed a significant energy storage and release, with a temperature increase of up to 6.3 °C. This work lays the foundation for a new generation of solar thermal fuels (STFs), where energy capture and release can be precisely controlled by doping the molecular photoswitch into the host LC matrices.</p>
30.	<p>Crack in presence of holes: Experimental measurements and configurational force analysis R Upadhyaya, S Sunil, RN Singh, A Tiwari - Theoretical and Applied Fracture Mechanics, 2025</p> <p>Abstract: The presence of holes significantly influences crack growth in elastic–plastic materials under monotonic loading. This study investigates the effect of holes on crack propagation in SS304 by evaluating the J-integral. A modified approach is developed to derive a geometry-dependent $f(a/W)$ function for $J_{elastic}$, while revised factors η and γ improve the accuracy of $J_{plastic}$ for nonstandard geometries. Finite element simulations using configurational forces provide additional insights into the crack driving force. This study enhances predictive capabilities for crack growth behavior in engineering applications</p>
31.	<p>Dark epiphany: The Lovecraftian in twentieth-century existential literature D Ray, S Gupta - Horror Studies, 2025</p> <p>Abstract: This article explores a convergence between H. P. Lovecraft’s cosmic horror fiction and twentieth-century existentialist literature. The point of convergence, we argue, is a moment in the narrative marked by the realization of human insignificance and purposelessness before an overwhelming ‘cosmic’, often resulting in unconditional surrender and incessant despair within the characters – we call it the ‘dark epiphany’. Our article, divided into two parts, will begin with an investigation of the aforementioned epiphanic moments in Lovecraft’s short stories, carefully tracing a gradual progression in their intensity and impact. The second half of the article will discuss the seminal works of Franz Kafka, Albert Camus and Jean-Paul Sartre to ascertain the unmistakable presence of a progressively increasing dark epiphany in these narratives. In the process, we attempt to draw parallels between the two strands of fiction, discuss their ideological overlaps and raise pertinent questions concerning the ‘cosmic’ and the ‘existential’.</p>
32.	<p>Development of a bovine gelatin-kappa carrageenan-based dual network biomimetic hydrogel for chondrogenic differentiation of mesenchymal stem cells A Mukherjee, J Rajput, A Poundarik, B Das - International Journal of Biological Macromolecules, 2025</p> <p>Abstract: Direct stem cell delivery for cartilage tissue engineering faces significant drawbacks, including loss of cells via circulation and poor viability in a hostile microenvironment. Hence, scaffold-based approaches for stem cell delivery are gaining significant momentum. In this study, composite hydrogel films composed of gelatin and κ-carrageenan dually crosslinked with glutaraldehyde and potassium chloride have been developed through the solvent casting method. The protein-polysaccharide composite mimics the natural extracellular matrix of native cartilage and the synergistic effects of covalent and ionic crosslinking provide mechanical strength, stability, and satisfactory biological performance. The physicochemical properties of the composite were analyzed using SEM-EDS, AFM, FTIR, XPS, and XRD. Rheological analysis revealed self-healing properties of the film and mechanical analysis demonstrated the ultimate tensile strength to be 13.49 ± 2.89 MPa, which mechanically mimics the native cartilage. The composite film remained stable for approximately 4 weeks in PBS, validating its stability. Biological assessments of the film after 7 days of culture demonstrated its long-term cytocompatibility, showing cell viability of 97.56 ± 0.21 %, cell adhesion was observed using</p>

FESEM micrographs, and cell proliferation through Live/Dead assay. The dually crosslinked biomimetic composite films aided in chondrogenic differentiation, as confirmed using collagen II staining and TGF- β expression studies, and hence demonstrate promising potential for cartilage tissue regeneration.

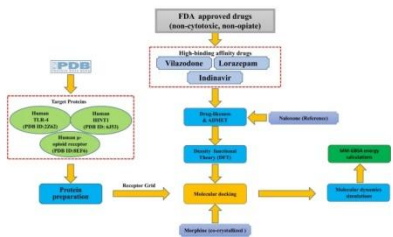


[Drugs repurposed against morphine and heroin dependence: molecular docking, DFT, MM-GBSA-based MD simulation studies](#)

JA Malik, MA Wani...JN Agrewala - In Silico Pharmacology, 2025

33.

Abstract: Morphine and heroin dependence are growing concerns worldwide. Drug dependence is one of the greatest challenges, and developing alternative therapeutic strategies is essential. Due to few treatment options in pain management, morphine, a potent analgesic, is widely prescribed, but it carries a high risk of abuse. For the management of drug dependence, we have limited treatment options available, therefore, strategies should be developed to manage drug-seeking behaviors in clinical settings. We tried to find any FDA-approved drug targeting μ -opioid receptors through the *in-silico* approach. We screened around 186 FDA-approved drugs; we observed several drugs showing better docking scores with good affinity. We found vilazodone, indinavir, and lorazepam as potential drugs based on their affinity and mechanism of action. Later, these drugs were screened against human μ -opioid (PDB ID:8EF6) and other novel drug targets (5HT1 and TLR-4) that are associated with morphine dependence. Following docking, density functional theory (DFT), molecular dynamics (MD), molecular mechanics, and general born surface area (MM-GBSA) were performed to calculate the stability and ligand–protein binding free energies. Vilazodone, indinavir and lorazepam showed promising docking, MD, the energy gap between the HOMO and LUMO chemical reactivity, and MM-GBSA results compared to morphine and naloxone. We propose that these three drugs have huge potential to reverse the morphine and heroin dependence in diseased subjects near future.



[Effect of carbon nanodots on the cellular redox reaction and immune system](#)

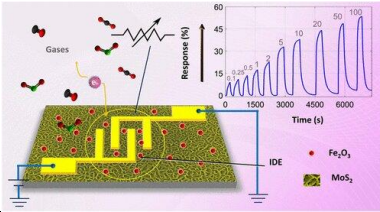
S Verma, M Bhatt, B Das - Nanoscale Advances, 2025


34.

Abstract: Carbon nanodots are ultra-small carbonaceous nanostructures with excellent photoluminescence and cytocompatibility properties, making them suitable for developing excellent bioimaging probes. They exhibit dual properties, generating and scavenging reactive oxygen species, and are used as photosensitizers to produce reactive oxygen species under light and as photothermal agents that transform light energy into heat. This makes it possible to use them in photothermal and photodynamic therapies to treat cancer. They may enter the body by various means, including inhalation, ingestion, or intravenous injection. Once inside, they travel through the bloodstream, infiltrating tissues where they come into contact with the immune system, similar to infectious agents. These nanodots are identified by several receptors on the surface of innate immune cells, such as monocytes and macrophages, which attempt to engulf these nanodots. This interaction can induce a pro-inflammatory (M1) or anti-inflammatory (M2)

	<p>response, modulating immune activity. This review explores the immuno-toxic potential of carbon nanodots, focusing on their ability to modulate redox balance by catalase, glutathione peroxidase, and superoxide dismutase, which are examples of antioxidant enzymes. Although carbon nanodots have demonstrated a wide range of applications, their effect on the cellular immune system remains largely unexplored. In this study, we primarily addressed the sophisticated impacts of carbon nanodots on the immune system and their diverse processes, such as the many cellular redox reactions implicated in antibacterial and antiviral treatment, wound healing, drug administration, and tumor therapy. As a result, we outline the benefits and difficulties of carbon nanodots in the biomedical domain and discuss their potential in the future development of clinical medicine.</p>
35.	<p>Effect of seabed geometry on the hydrodynamic performance of a thick wavy porous barrier V Venkateswarlu, DS Kumar... SC Martha - Journal of Marine Science and Application, 2025</p> <p>Abstract: This study evaluates the physical mechanisms of incident waves as they interact with a porous wavy barrier of finite thickness. A wave-trapping chamber is formed between the thick wavy barrier (TWB) and partially reflecting seawall (PRS). The effect of seabed undulations is incorporated into the wave-trapping analysis of the TWB. The boundary value problem proposed in this study is solved using a multidomain boundary element method within the context of linear potential flow theory. Coefficients such as reflection, runup, horizontal force on PRS, and vertical force on TWB are examined for various structural configurations. The position of seabed undulations is analyzed for four scenarios: i) seabed undulations upwave of the wavy barrier with a trapping chamber, ii) seabed undulations upwave of the wavy barrier without a trapping chamber, iii) seabed undulations underneath the wavy barrier with a trapping chamber, and iv) seabed undulations beneath the wavy barrier without a trapping chamber. The study results are compared with known results to verify their accuracy. The effects of PRS, TWB porosity, trapping chamber, plate thickness, seabed type, and submergence depth on hydrodynamic coefficients are analyzed against relative water depth. The study reveals that the introduction of a porous TWB with a trapping chamber results in minimal hydrodynamic coefficients (reduced reflection and force on a wall) compared to a rigid TWB without a trapping chamber. A comparison of various seabeds is reported for all combinations of TWB with a chamber. The sloping seabed upwave of the barrier with a trapping chamber, 20% plate porosity, and 50% wall reflection at an appropriate submergence depth could replace gravity-type breakwaters in deeper waters. This study holds great potential for analyzing wave trapping coefficients by TWB to provide an effective coastal protection system.</p>
36.	<p>Efficient implementations of a Born Series for computing photoacoustic field from a collection of erythrocytes U Mandal, N Singh, K Singh, VN Hagone, J Singh... - Photoacoustics, 2025</p> <p>Abstract: Numerical implementation of the Born series procedure is a computationally expensive task. Various computational strategies have been adopted and tested in this work for fast execution of the convergent Born series (CBS) algorithm for solving inhomogeneous Helmholtz equation in the context of biomedical photoacoustics (PAs). The PA field estimated by the CBS method for a solid circular disk approximating a red blood cell exhibits excellent agreement with the analytical result. It is observed that PA pressure map for a collection of red blood cells (mimicking blood) retains the signature of multiple scattering of acoustic waves by the acoustically inhomogeneous PA sources. The developed numerical tool realizing the CBS algorithm compatible with systems having multiple graphics processing units can be utilized further for accurate and fast estimation of the PA field for large tissue media.</p>
37.	<p>Epilepto: An epilepsy self-management app R Shukla, RS Krishnu, VP Nathasha, G Singh, AK Sahani - IETE Technical Review, 2025</p> <p>Abstract: Persons with epilepsy (PWE), faces many challenges during treatment, like</p>

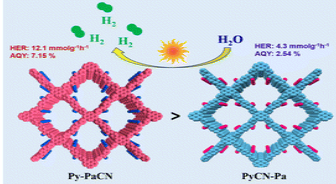
	<p>maintaining medication adherence, proper documentation of seizure details, limited understanding of the disease, fear of helplessness on seizure occurrence, and stigma. A complicated medication regimen also creates issues in patients, especially those with limited education. It becomes difficult for the physicians to ensure medication adherence in the patient and adequately understand treatment effects without detailed information of seizures. We have hypothesized that a mobile application can improve medication adherence and epilepsy self-management (ESM) skills. We have developed an Epilepto App with seizure diary, medicine reminder, prescription recorder, caregiver alert, epilepsy educational content, chatbot, and video recording features. These features of the App will improve medication adherence and ESM and facilitate physicians to understand the efficacy and any side effects of treatment. The App is developed on the input of medical experts; it is designed so that people with limited education can also use it easily. App can be used in any Indian regional language. A usability testing and satisfaction survey was conducted on nine PWE. Nearly all the subjects were able to use the app feature; the most liked features were medication adherence, seizure diary, and alert to caregiver.</p>
38.	<p>Experimental and numerical investigation on heat dissipation capability of micro-pillar textured cutting tools G Saraf, G Sharma, R Kumar, CK Nirala - Scientific Reports, 2025</p> <p>Abstract: In metal cutting, the extreme tool temperature restricts the material removal rate. To address this, it is crucial to adopt techniques that reduce heat input and enhance heat dissipation from the cutting tool inserts. Rake surface texturing, particularly with micro-pillars, is gaining popularity in this context. Direct measurement of the cutting tool temperature is exceptionally challenging, so a numerical approach is adopted in this work to inverse estimate the tool tip temperature based on the temperature measured at a distant location from the rake face. Stage I of the work involved the development of a circular micro-pillar array on tungsten carbide inserts using the Reverse Micro Electrical Discharge Machining (RμEDM) technique. Based on the discharge pulses recorded during RμEDM, the 110V–100 nF voltage-capacitance combination proved feasible for this operation. In Stage II, turning operations were performed on Ti6Al4V alloys under dry, compressed air, and wet conditions. The tool temperature measured at the distant location revealed a substantial temperature drop for textured tools. This is attributed to the reduced contact area at the interface, as observed from the rake morphology of the tools, and to the enhanced heat dissipation from the higher surface area of the developed textures, as revealed by the computational fluid dynamics-based numerical study in Stage III of the work. An array of closely spaced, small-diameter, and higher-depth micro-pillars beyond the tool-chip contact area could enhance heat dissipation from the cutting tools.</p>
39.	<p>Fe₂O₃-functionalized MoS₂ nanostructure sensor for high-sensitivity and low-level SO₂ detection R Gond, S Barala, P Shukla, G Bassi, S Kumar, M Kumar...B Rawat - ACS sensors, 2025</p> <p>Abstract: Real-time sulfur dioxide (SO₂) monitoring is essential to mitigate its severe health and environmental impacts while ensuring compliance with industrial safety and emission regulations. Two-dimensional MoS₂ stands out as a promising material for developing low-temperature-operated gas sensors due to its exceptionally high surface-to-volume ratio and ease of surface functionalization. However, monitoring the SO₂ level faces challenges, including limited selectivity, sensitivity, and detection range, with high operating temperatures (200–600 °C) or external light source requirements. To address these issues, we present a highly sensitive SO₂ sensor based on Fe₂O₃ nanoparticle-functionalized vertically aligned MoS₂ nanostructure material, which is fabricated using a scalable sputtering process. The Fe₂O₃–MoS₂ sensor exhibits a broad detection range from 100 ppb to 100 ppm, with a theoretical detection limit of around 22.8 ppb. When exposed to 5 ppm of SO₂, the sensor achieves a response of around 32.2%, with response and recovery times of approximately 104 and 141 s, respectively. The fabricated sensor demonstrated impressive sensitivity (4.9%/ppm) for SO₂ concentration in the range of 0.1 to 5 ppm, coupled with excellent reproducibility and stability at 150 °C. This</p>

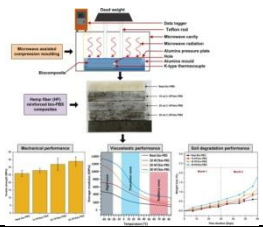
	<p>enhanced performance is attributed to the catalytic effect of Fe_2O_3 and modulation of the heterojunction barrier at the interface. This study introduces a highly scalable, reliable, and stable Fe_2O_3-MoS_2 sensor, which paves the way for developing energy-efficient and miniaturized SO_2 sensors.</p> 
40.	<p>Generation of structured light and controlled-NOT gate in microwave regime P Bhardwaj, S Dasgupta - Applied Physics B : Lasers & Optics, 2025</p> <p>Abstract: We propose how to generate beams with non-zero orbital angular momentum in the microwave domain using atomic vapor medium and coherent control techniques. Our approach utilizes a difference frequency generation process in a centrosymmetric medium in the presence of a DC electric field for frequency conversion and parametric amplification. By employing phase matching conditions and orbital angular momentum conservation, we constructed a Controlled NOT gate using a three-level atomic configuration. By generating Laguerre-Gaussian fields in the microwave domain, we open up novel possibilities for advanced information processing in wireless communication and potential applications in quantum technologies.</p>
41.	<p>Granular ball K-Class twin support vector classifier MA Ganaie, V Ahire, A Girard - Pattern Recognition, 2025</p> <p>Abstract: This paper introduces the Granular Ball K-Class Twin Support Vector Classifier (GB-TWKSVC), a novel multi-class classification framework that combines Twin Support Vector Machines (TWSVM) with granular ball computing. The proposed method addresses key challenges in multi-class classification by utilizing granular ball representation for improved noise robustness and TWSVM's non-parallel hyperplane architecture solves two smaller quadratic programming problems, enhancing efficiency. Our approach introduces a novel formulation that effectively handles multi-class scenarios, advancing traditional binary classification methods. Experimental evaluation on nine UCI benchmark datasets demonstrates that GB-TWKSVC significantly outperforms state-of-the-art classifiers in both accuracy and computational performance, achieving up to 5% higher accuracy and 50% faster computation than Twin-KSVC and 1-versus-rest TSVM. Notably, it attains 99.34% accuracy on Iris and 91.04% on Ecoli, surpassing competing methods. The method's effectiveness is validated through comprehensive statistical tests and complexity analysis, establishing a mathematically sound framework. The results highlight GB-TWKSVC's potential in pattern recognition, fault diagnosis and large-scale data analytics utilizing its ability to capture fine-grained features in high-dimensional data making it a valuable advancement in classification algorithms.</p>
42.	<p>Hardness results and approximability of cosecure domination in graphs. Kusum, A Pandey - Discrete Mathematics, Algorithms and Applications, 2025</p> <p>Abstract: Let $G=(V,E)$ be a simple graph with no isolated vertices. A dominating set S of G is said to be a cosecure dominating set of G, if for every vertex $v \in V$ there exists a vertex $u \in V \setminus S$ such that $uv \in E$ and $(S \setminus \{v\}) \cup \{u\}$ is a dominating set of G. The Minimum Cosecure Domination problem is to find a minimum cardinality cosecure dominating set of G. In this paper, we show that the decision version of the problem is NP-complete for split graphs, undirected path graphs (subclasses of chordal graphs), and circle graphs. We also present a linear-time algorithm to compute the cosecure domination number of cographs (subclass of circle graphs). In addition, we present a few results on the approximation aspects of the problem.</p>

43.	<p>High-performance paper-based DNA-conjugated $\text{Ti}_3\text{C}_2\text{T}_x$ bio-nanoelectrode for rapid point-of-care detection of HPV-16 R Rawat, S Singh, R Walia... - IEEE Sensors Journal, 2025</p> <p>Abstract: Cervical cancer remains a significant global health concern, with high-risk human papillomavirus (HR-HPV), particularly the genotype 16, identified as a key etiological factor with a significantly high mortality rate. The conventional diagnostic methods suffer from limitations related to efficiency and affordability, thereby necessitating the development of novel miniaturized biosensing platforms. In this study, we present the creation of an electroanalytical genosensor utilizing $\text{Ti}_3\text{C}_2\text{T}_x$/DNA hybrid screen-printed paper electrode strips for the detection of cervical cancer, based on varying concentrations of HPV-16. The Mxene nanostructures were characterized using X-ray diffraction (XRD), field-emission scanning electron microscopy (FESEM), Fourier transform infrared (FTIR) spectroscopy, and UV-visible (UV-Vis) spectroscopy. The performance of the bionanoelectrode toward HPV-16 detection was examined using cyclic voltammetry (CV) analysis. The sensitivity and limit of detection (LoD) were calculated to be $1.65 \mu\text{A/fM/mm}^2$ and 2.4 fM, respectively, while demonstrating selectivity to HPV-16 DNA and generating a shelf life of ~1 month. The developed bionanoelectrode was further integrated with miniaturized electronics and 3-D printing technology, and the resulting device—Cervicare demonstrated appreciable performance (LoD = 0.02 pM). This indicates significant potential of the developed Cervicare device for implementation in point-of-care (PoC) scenario, toward providing affordable healthcare among the affected populace.</p> 
44.	<p>ILAM: Cross-fusion of latent and attention features for explainable medical image classification A Sharma, U Varman, V Bharti, A Kumar, AK Singh, SK Singh - IEEE Journal of Biomedical and Health Informatics, 2025</p> <p>Abstract: Accurate and interpretable AI models play a critical role in medical image analysis. However, despite advancements in explainable AI (XAI), existing methods struggle with inconsistent interpretability. To overcome this limitation, we introduce the Integrated Latent and Attention Mapping (ILAM) framework, which enhances both classification accuracy and explainability by fusing local and global feature representations. ILAM integrates a custom-designed Autoencoder (AE) with a Vision Transformer (ViT), where the AE learns fine-grained local features through unsupervised patchwise image reconstruction in the latent space. These local features are then fused with global representations extracted by ViT, creating a hybrid model that improves both performance and post hoc interpretability. To refine explainability, ILAM incorporates a modified attention rollout mechanism, which recursively aggregates latent feature representations and attention weights to produce precise and stable activation maps. We evaluate ILAM on three publicly available medical imaging datasets—BreakHis, Chest X-Ray, and Retinal, demonstrating its superior performance over transformer-based models such as ViT, DeiT, CvT, and SwinT. ILAM consistently generates detailed and reliable activation maps, providing clearer visualizations of critical image regions influencing model decisions. By effectively combining local and global feature fusion, ILAM establishes itself as a robust and interpretable framework for medical image classification.</p>
45.	<p>Impact of EMI on the reliability of crossbar architecture-based inference in CMOS technology Shivdeep, S Boyapati, DM Das - IEEE Transactions on Components, Packaging and Manufacturing Technology, 2025</p>

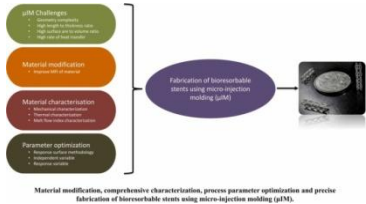
	<p>Abstract: Electromagnetic Interference (EMI) can compromise the accuracy of inference and, hence, the reliable decision-making of an AI-based autonomous circuit. The summing amplifier at the crossbar's output converts the weighted sum of currents into voltage. Amplifiers are inherently susceptible to EMI, which induces a DC offset at the output, leading to incorrect summation. This can potentially compromise the reliability of crossbar-based hardware implementing artificial intelligence for mission-critical applications. This paper investigates the EMI susceptibility of amplifiers and crossbar circuits. We have designed the crossbar circuit of size 2×2 using 180 nm CMOS technology to show the EMI-induced offset, considering resistive weights. The effect of weights of the crossbar circuit on the EMI susceptibility is discussed. The EMI-immune amplifier and crossbar circuit design to achieve immunity without trading off the area, power, and complexity is proposed, as these are critical parameters for large crossbar circuits. The problem is illustrated by implementing the 2×2 crossbar circuit with commercial OpAmp ICs. A 7-segment digit recognition application is implemented on a 7×10 crossbar to illustrate the incorrect inference due to EMI susceptibility and made EMI-immune.</p>
46.	<p>Impact of equipment material and surface finish on the flowability of dry cohesive powders—an important consideration in calibration of discrete element models A Sharma, J Chakraborty, A Tripathi, J Kumar, M Sen, W Ketterhagen - Journal of Pharmaceutical Innovation, 2025</p> <p>Abstract: Discrete Element Method (DEM) simulations of cohesive particles are of great importance in understanding powder flows in processing equipment. Calibration of the particle–particle or particle–wall interaction parameters is important, and although there are many studies on DEM simulations of cohesive powders, most of them do not differentiate between particle–particle cohesive and particle–wall adhesive forces. In this work, a bench-top experimental setup was designed to demonstrate the effect of particle–wall adhesive forces. A simulation-based sensitivity analysis was also performed using a commercial scale tablet press feeder (TPF) and hopper screw feeder (HSF), by independently varying the particle–particle and particle–wall cohesive energy density values to illustrate their effect on powder flowability. Both the feeders experienced blockages for highly cohesive particles whose cohesive energy density exceeds 80 kJ/m³ in case of TPF and 110 kJ/m³ for HSF. The occurrence of such blockages was eliminated by reducing the particle–wall adhesion to 30 kJ/m³ in case of TPF and 50 kJ/m³ for HSF while keeping the particle–particle cohesion at the same high value. Thus, this work demonstrates that the particle–particle cohesion and particle wall adhesion should be considered as separate entities and must be calibrated separately in DEM so that the materials interaction effects of both powder and equipment can be captured adequately.</p>
47.	<p>Influence of clamp pressure on weld performance and fracture mode in laser welded polyamide-6 sheets DK Goyal, A Bajpai, R Kant - Materials Letters, 2025</p> <p>Abstract: This study investigates the effect of clamp pressure on laser transmission welding of polyamide-6 sheets using electrolytic iron powder for energy absorption. Welding is performed with a fibre laser on 2 mm thick polyamide-6 sheets, and the influence of clamp pressure on weld strength and morphology is analysed. Results show that weld strength increases with pressure up to an optimal level but decreases beyond due to excessive molten polymer loss. SEM analysis confirms iron particle embedding, enhancing mechanical interlocking. Fractographic analysis shows substrate and interface fracture patterns with pressure variations, indicating differences in molecular interdiffusion. The findings highlight the importance of optimizing clamp pressure for better joint strength and integrity.</p>
48.	<p>Influence of nano rice husk ash on geotechnical properties of black cotton soil NJ Sahare, M Raheena - Indian Geotechnical Journal, 2025</p> <p>Abstract: Black cotton soil's notable swelling and shrinkage contribute to structural damage.</p>

	<p>This study examines the impact of nano rice husk ash (nRHA) variants on this soil: One synthesized in 60 h and another through 7 h combined dry–wet milling method. The primary objective is to assess the effects of nRHA treatment on the soil's index properties, engineering characteristics and swelling behavior. Laboratory tests including free swell index, Atterberg's limits, swelling potential, swelling pressure, unconfined compressive strength and consolidation tests were conducted on black cotton soil samples treated with both nRHA variants. Results indicated that the 7-h nRHA treatment led to lower plasticity and reduced swelling compared to the 60-h variant. Specifically, the 7-h treated soil showed decreased swelling pressure, compression index and rate of primary swelling, along with increased pre-consolidation pressure and unconfined compressive strength. The free swell index also decreased by 21% with the 7-h nRHA treatment. The superior performance of the 7-h milled nRHA is likely due to its higher calcium and reactive silica content, enhancing its stabilizing effect. This research highlights the 7-h nRHA as a more effective stabilizer for black cotton soil, offering a promising solution to mitigate its problematic volumetric behavior.</p>
49.	<p>Influence of pressure on the properties of the multigap type-I superconductor BeAu R Khasanov, R Vocaturo, O Janson, A Koitzsch, R Gupta, D Das, NPM Casati, MG Vergniory, JVD Brink, E Svanidze - <i>Physical Review B</i>, 2025</p> <p>Abstract: We report on studies of the superconducting and normal-state properties of the noncentrosymmetric superconductor BeAu under hydrostatic pressure conditions. The room-temperature equation of state (EOS) reveals the values of the bulk modulus (B_0) and its first derivative (B_0') at ambient pressure to be $B_0 \approx 133 \text{ GPa}$ and $B_0' \approx 30$, respectively. Up to the highest pressures studied ($p \approx 2.2 \text{ GPa}$), BeAu remains a multigap type-I superconductor. The analysis of $B_c(T, p)$ data within the self-consistent two-gap approach suggests the presence of two superconducting energy gaps, with the gap-to-T_c ratios $\Delta_1/kBT_c \sim 2.3$ and $\Delta_2/kBT_c \sim 1.1$ for the larger and smaller gaps, respectively [$\Delta = \Delta(0)$ is the zero-temperature value of the gap and k_B is the Boltzmann constant]. With increasing pressure, Δ_1/kBT_c increases while Δ_2/kBT_c decreases, suggesting that pressure enhances (weakens) the coupling strength between the superconducting carriers within the bands where the larger (smaller) superconducting energy gap has opened. The superconducting transition temperature T_c, the zero-temperature values of the superconducting gaps Δ_1 and Δ_2, and the zero-temperature value of the thermodynamic critical field $B_c(0)$ decrease with increasing pressure, with the rates of $dT_c/dp \approx -0.197 \text{ K/GPa}$, $d\Delta_1/dp \approx -0.034 \text{ meV/GPa}$, $d\Delta_2/dp \approx -0.029 \text{ meV/GPa}$, and $dB_c(0)/dp \approx -2.65 \text{ mT/GPa}$, respectively. The measured $B_c(0)$ values plotted as a function of T_c follow an empirical scaling relation established for conventional type-I superconductors.</p>
50.	<p>Iodine-mediated peptide disulfide bridging is reversible and sequence-dependent in solid support: Use of TEMPO in the reaction resolves the challenge A Chowdhury, NM Tripathi, N Verma, S Ghosh, B Pati, A Bandyopadhyay - <i>Asian Journal of Organic Chemistry</i>, 2025</p> <p>Abstract: Iodine (I_2) is an extremely popular reagent for disulfide assembly in solution, solid phase (pseudo-dilute conditions) peptides, and immobilized materials. However, we noticed that I_2-mediated peptide disulfide assembly often resulted in incomplete reactions due to its redox activity under pseudo-dilute conditions. The phenomenon intrigued us to conduct an in-depth analysis of I_2-mediated disulfide assembly with various peptide sequences. We revealed that the redox equilibrium between free thiols and disulfide products was peptide sequence-dependent and previously unsolicited. Adding TEMPO in the reaction medium attenuates the I_2-mediated redox equilibrium and rapidly ($\sim 5 \text{ min}$) promotes quantitative, clean disulfide assembly. Finally, in silico investigations supported that this chemical equilibrium primarily relies upon the increased global free energy upon macrocyclization and the interspace between thiol groups in the linear peptide chain. This fundamental study will leverage multiple advantages in disulfide</p>

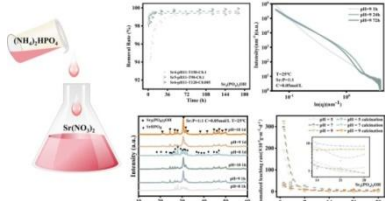
	formation in immobilized materials and peptide modification chemistries with iodine in solid support.
51.	<p>Isomeric cyano-vinylene-linked covalent organic frameworks and their impact on photocatalytic hydrogen evolution A Nagar, A Alam, P Pachfule, CM Nagaraja - Journal of Materials Chemistry A, 2025</p> <p>Abstract: Covalent organic frameworks (COFs) can be precisely designed through the choice of organic building blocks, bridging linkages and topologies with tailored photophysical properties, which consequently leads to their significantly different photocatalytic performances. Besides, the orientation of the bridge linkages in the COF backbone plays a critical role in facilitating photogenerated charge separation and migration and is one of the most important factors for photocatalysis. Herein, we demonstrate a pair of constitutionally isomeric cyano-vinylene-linked COFs (Py-PaCN and PyCN-Pa) with the same composition but different atomic arrangements of cyano-vinylene linkages to unveil their insightful structure–activity relationship for photocatalytic hydrogen generation <i>via</i> water splitting. The hydrogen evolution rate of Py-PaCN COF reaches up to 12.1 mmol g⁻¹ h⁻¹ (AQY = 7.15%), which is about three times higher than that of its isomer PyCN-Pa COF with 4.3 mmol g⁻¹ h⁻¹ (AQY = 2.54%), using ascorbic acid as a sacrificial agent. These minor structural changes in COFs result in remarkable variations in their light-harvesting, optoelectronic, and redox properties, resulting in divergent photocatalytic hydrogen evolution activity. This investigation of the constitutional isomerism of linkages in COFs will help in the selection of the right building blocks with distinct functionality in the design and precise tuning of the photophysical properties of COFs.</p> 
52.	<p>J-contractive operator valued functions, vector valued de Branges spaces and functional models B Garg, S Sarkar - Journal of Mathematical Analysis and Applications, 2025</p> <p>Abstract: The aim of this paper is to study the vector valued de Branges spaces, which are based on <i>J</i>-contractive operator valued analytic functions, and to explore their role in the functional models for simple, closed, densely defined, symmetric operators with infinite deficiency indices.</p>
53.	<p>Lightweight aluminum joint design: Enhancement of mechanical properties through novel inter-layer and powder additives in friction stir welding E Ahmed, M Muaz, S Arif, R Kant... - International Journal of Lightweight Materials and Manufacture, 2025</p> <p>Abstract: Friction Stir Welding (FSW) is a solid-state joining technique that has garnered significant attention for its ability to weld aluminum alloys while mitigating common issues such as porosity and thermal defects inherent in fusion welding. This study systematically evaluates the impact of inter-layers and powder additives on the mechanical properties of aluminum FSW joints. Magnesium (Mg) ribbons and Lead–Tin (Sn–Pb) alloy ribbons were employed as inter-layers, while Boron Carbide (B₄C), Titanium Dioxide (TiO₂), and Manganese (Mn) served as reinforcement powders. Quantitative analysis demonstrated that the combination of Manganese (Mn) powder and Sn–Pb alloy inter-layer achieved a remarkable 28 % improvement in hardness, a 35 % reduction in wear rate, and a 42 % increase in shear strength. Additionally, Mn powder alone yielded the highest shear strength, while Sn–Pb inter-layer with Mn powder provided maximum hardness and wear resistance. Mg ribbon combined with Mn powder produced the lowest surface roughness. These enhancements were corroborated by mechanical testing and morphological characterization, including scanning electron microscopy (SEM), energy-</p>

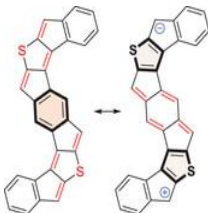
	<p>dispersive X-ray spectroscopy (EDS), and microstructural mapping. The findings highlight the effectiveness of tailored inter-layer and powder combinations in enhancing weld quality, providing insights into the underlying mechanisms responsible for these improvements. This study underscores the industrial relevance of these advancements, offering transformative potential for sectors such as aerospace and automotive manufacturing where superior joint properties are critical.</p>
54.	<p>Macroeconomic impact of demographic transition and effectiveness of monetary policy: Evidence from East Asian economies K Rai, B Garg - Emerging Markets Finance and Trade, 2025</p> <p>Abstract: This article examines the impact of changing age structure on selected macroeconomic indicators and the effectiveness of monetary policy transmission. We use the panel of nine East Asian economies from 1990 to 2020 and employ a dynamic common correlated effects estimator. The results indicate that the working-age population, particularly the prime working-age cohort, emerges as a key driver of economic growth and savings. However, the growing old-age dependency rate poses significant challenges by reducing aggregate saving and diminishing the effectiveness of monetary policy. Overall, financial institutions play a critical role, amplifying the positive effects of workforces on saving, while young working age significantly improves the monetary policy transmission effectiveness.</p>
55.	<p>Mechanical, viscoelastic and soil degradation performance of hemp fiber reinforced bio-PBS composites developed via microwave processing A Sharma, S Zafar, CK Nirala - Fibers and Polymers, 2025</p> <p>Abstract: This study focuses on bio-based natural fiber-reinforced polymer composites (NFRPCs). In this work, bio-polybutylene succinate (bio-PBS) reinforced with hemp fibers (HF) varying at 10 wt%, 20 wt%, and 30 wt% were developed via microwave-assisted compression moulding (MACM) technique. The mechanical properties, crystalline properties, dynamic mechanical analysis, and soil degradation behaviour of these composites were analysed. The study demonstrated that composites with 30 wt% hemp fiber content exhibited the most optimal mechanical properties, with crystallinity increasing by 22%. These composites achieved the highest storage modulus of 13,349 MPa, while their loss modulus was found to be 110% higher compared to neat bio-PBS. Additionally, soil burial experiments revealed that the 30 wt% HF/bio-PBS composites underwent the greatest weight loss after 60 days of soil exposure, indicating superior biodegradability compared to the pure bio-PBS matrix. The work further concluded that hemp fiber-reinforced bio-PBS composites showcased improved mechanical performance, crystallinity, biodegradability, and processing characteristics, surpassing other bio-composite alternatives.</p> 
56.	<p>Mitigating ecological tipping points via game–environment feedback A Mandal, S Sarkar, S Chakraborty, PS Dutta - Proceedings of the Royal Society A: Mathematical, Physical and Engineering Sciences, 2025</p> <p>Abstract: Widespread exploitation of biological resources raises concerns about the emergence of tipping points characterizing abrupt ecosystem collapse. Mitigating these tipping points is crucial for the sustainability of our being. However, our understanding of how the feedback loop between human exploitation strategies and the environment influences the mechanisms governing these tipping points remains elusive. This study employs an eco-evolutionary game-</p>

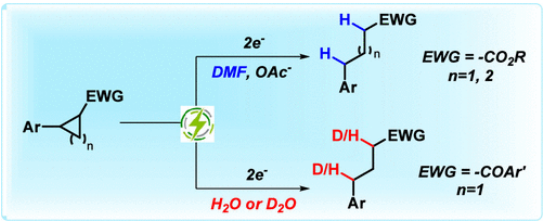
	<p>theoretic framework to explore the coupled dynamics of a renewable resource undergoing a sudden collapse. We investigate the co-evolution of strategic interactions and environmental dynamics using six possible game combinations representing diverse social dilemmas. We find that, depending on the choice of environment-dependent payoff structure, the tipping point can be shifted or even completely eluded. Additionally, this study emphasizes the impact of monitoring and punishment mechanisms against high-effort exploitation strategists on the system's resilience. Our results unveil a rich spectrum of dynamics, spanning from multi-stability to oscillation, thereby presenting formidable challenges to resource management. While addressing the tragedy of the commons resulting from heightened harvesting efforts, targeted penalties for high-effort strategists emerge as a mitigating factor. Overall, our study highlights the interplay between ecological tipping points, individual decision-making and external control mechanisms within the realm of resource management.</p>
57.	<p>Mixed functionalization as a pathway to induce superconductivity in MXenes: Vanadium and niobium carbide P Jamwal, R Ahuja, R Kumar - Physical Chemistry Chemical Physics, 2025</p> <p>Abstract: The functionalization versatility of MXenes distinguishes them from other two-dimensional materials, enabling the design of numerous new materials with unique properties. By leveraging surface chemistry, functionalization allows for the manipulation of critical parameters such as the density of states and electron-phonon coupling, providing an excellent platform for exploring two-dimensional superconductivity. In this study, we investigate the impact of functionalization on Vanadium Carbide (V_2C) MXene, which is intrinsically non-superconducting, by considering three different cases: (i) hydrogen adatoms, (ii) fluorine adatoms, and (iii) mixed functionalization with hydrogen and fluorine adatoms. We confirm the mechanical and dynamical stability of functionalized V_2C using Born's stability criteria and phonon dispersion analyses. In all three cases, superconductivity emerges due to the presence of functional groups, which influence the electron-phonon interaction and electronic structure, leading to an enhanced electron-phonon coupling constant. The highest superconducting transition temperature is observed for mixed-functionalized V_2C, attributed to the softening of the ZA phonon mode along with high-energy phonon modes induced by hydrogen. To further explore the potential of mixed functionalization in inducing superconductivity, we extend our approach to another non-superconducting MXene, Nb_2C. The mixed-functionalized Nb_2C exhibits a superconducting transition temperature of 9.2 K, which surpasses the reported values for Nb_2CH_2, Nb_2CS_2, and Nb_2CBr_2. These findings underscore the effectiveness of mixed functionalization in enabling superconductivity in MXenes, paving the way for future theoretical and experimental investigations.</p>
58.	<p>Multilane bidirectional traffic in a strongly coupled exclusion model with constraint resources AK Pandey, A Gupta, AK Gupta - Physical Review E, 2025</p> <p>Abstract: Motivated by complex bidirectional transport processes that occur in various biological and physical systems, we examine a one-dimensional closed system comprising two parallel lanes under limited resources. One lane is characterized by driven diffusive transport, while the other supports solely unidirectional motion in the opposite direction, mutually coupled through strong coupling. The total number of particles in the system, quantified by the filling factor, regulates the inflow of particles onto the lanes. The stationary properties of the system are analyzed through both simple and vertical cluster mean-field approaches, complemented by boundary layer analysis to elucidate its detailed behavior. Our theoretical results demonstrate that, for any set of parameters, one of the lanes invariably resides in a phase of zero net particle flux, manifesting either in a completely empty or fully jammed state. Two distinct types of phase transitions are identified and characterized: bulk transitions and surface transitions. Notably, phases emerge that exhibit boundary layers in their density profiles near both boundaries. A distinctive feature of the interplay between lane coupling and bidirectional transport is the</p>

	<p>appearance of kink and dip in the boundary layers, which is scrutinized by using the residence time method and fixed point analysis. Furthermore, we investigate the dynamics of phases involving shock and its sensitivity to system parameters. All theoretical outcomes are corroborated through stochastic simulations based on the Gillespie algorithm and numerical technique.</p>
59.	<p>Novel net-shape manufacturing of bioresorbable coronary stents using micro-injection molding process DK Tyagi, DK Mahajan - CIRP Journal of Manufacturing Science and Technology, 2025</p> <p>Abstract: The bioresorbable cardiovascular stent (BCS) represents a significant advancement in medical technology, offering temporary support to diseased arteries while eliminating the long-term risks associated with permanent implants. However, traditional fabrication methods involve multiple steps, rendering BCS a costly medical device. To address this challenge, net-shape manufacturing techniques have emerged as a promising approach to streamline production and facilitate mass manufacturing. Micro-injection molding (μIM) is a viable method for producing BCS with precise geometries and surface finishes. Yet, the inherent complexities of BCS geometry and the poor melt flow index (MFI) of material present significant obstacles to successful μIM fabrication. In this study, poly-lactic acid (PLA), was modified with triethyl citrate (TEC), a bio-based plasticizer, to enhance its MFI and processability. A comprehensive characterization of the PLA-TEC formulations was conducted, encompassing mechanical strength, thermal stability, and rheological behavior, to optimize material performance for μIM. Subsequently, process parameters were optimised utilising response surface methodology to mitigate manufacturing defects such as underfilling and flash formation, ensuring the production of high-quality BCS. Through systematic material modification and process optimization, this study successfully demonstrates the feasibility of μIM for cost-effective, high-volume production of BCS with improved geometric fidelity.</p>  <p>Material modification, comprehensive characterization, process parameter optimization and precise fabrication of bioresorbable stents using micro-injection molding (μIM).</p>
60.	<p>Pace in concert with phase: rate-induced phase-tipping in birhythmic oscillators R Kumar K, H Alkhayyon, S Wiczeorek, PS Dutta - Proceedings of the Royal Society A: Mathematical, Physical and Engineering Sciences, 2025</p> <p>Abstract: We study rate-induced phase-tipping (RP-tipping) between two stable limit cycles of a birhythmic oscillator. We say that such an oscillator RP-tips when a time variation of an input parameter preserves the bistability of the limit cycles but induces transitions from one stable limit cycle to the other, causing abrupt changes in the amplitude and frequency of the oscillations. Crucially, these transitions occur when: the rate of change of the input is in a certain interval bounded by <i>critical rate(s)</i>, and the system is in <i>certain phases</i> of the cycle. We focus on two illustrative examples: the birhythmic van der Pol oscillator and the birhythmic Decroly–Goldbeter glycolysis model, each subjected to monotone and non-monotone shifts in their input parameters. We explain RP-tipping in terms of properties of the autonomous frozen system, including the <i>phase</i> of a cycle and <i>partial basin instability</i> along the parameter path traced by the changing input. We show that RP-tipping can occur as an irreversible one-way transition or as a series of transitions between the stable limit cycles. Finally, we present RP-tipping diagrams showing combinations of the rate and magnitude of parameter shifts and the phases of the oscillation that give rise to this genuine non-autonomous instability.</p>
61.	<p>Performance analysis of active STAR-RIS-assisted NOMA with hardware impairments at finite</p>

	<p>blocklength S Kumar, B Kumbhani - Digital Signal Processing, 2025</p> <p>Abstract: The active simultaneously transmitting and reflecting-reconfigurable intelligent surface's (ASTAR-RIS) potential to avoid multiplicative fading loss by utilizing integrated reflection-type amplifiers has drawn considerable interest. This paper investigates the finite blocklength (FBL) analysis of ASTAR-RIS-assisted non-orthogonal multiple access (NOMA) with perfect and imperfect successive interference cancellation (SIC) in the presence of hardware impairments over cascaded Rician fading channels. Firstly, we derive the statistical distribution of cascaded Rician fading channels with the help of Laguerre polynomial series approximation. Secondly, we derive the novel analytical expression for average block error rate (ABLER), ergodic rate (ER), and system throughput with the help of the Gauss Chebyshev quadrature and the Gauss Laguerre quadrature method. Thirdly, the asymptotic expression for ABLER is derived to gain useful insights. Finally, the Monte Carlo simulations are used to verify the analytical results. Numerical results verify the correctness and superior performance of ASTAR-RIS-assisted NOMA (ASTAR-RIS-NOMA) over passive STAR-RIS-assisted NOMA (PSTAR-RIS-NOMA) and ASTAR-RIS-assisted orthogonal multiple access (OMA) (ASTAR-RIS-OMA). Additionally, the impact of other system parameters like imperfect SIC, hardware impairments, and block length are analyzed.</p>
62.	<p>PLA4MS: Curated georeferenced dataset for cloud removal in remote sensing S Ghildiyal, A Kumar, N Goel, M Saini, A El Saddik - IEEE Journal of Selected Topics in Applied Earth Observations and Remote Sensing, 2025</p> <p>Abstract: The presence of meticulously curated extensive training datasets plays a crucial role in advancing the performance of deep learning techniques that generalize well for extracting geoinformation from multisensor remote sensing imagery. Despite numerous datasets being published by the research community, a substantial portion of them are hampered by significant constraints, such as low spatial resolution, lack of ground details over time, and insufficient sample quantity. This article utilizes the openly accessible data obtained from the Planetscope satellites managed by Planet Labs. We have curated a dataset called PLA4MS comprising 64 557 pairs of images depicting cloudy and cloud-free conditions. The study focuses on the Ropar region of Punjab, India, as the primary area of interest, ensuring precise georeferencing at a spatial resolution of approximately 3 m across all meteorological seasons. This work presents a comprehensive cloud-removal dataset aimed at advancing remote sensing techniques, with cloud removal as the primary focus. This dataset is created to serve the research community, as it offers the potential to support broader remote sensing applications by enabling researchers to generate cloud-free images for time-series analysis, land cover land use classification, change detection, and other agricultural tasks.</p>
63.	<p>Response of ^{90}Sr precipitated into $\text{Sr}_5(\text{PO}_4)_3\text{OH}$ and SrHPO_4 by Wet-Chemistry: New insights into the phase evolution during grain growth D Yin, Q Zheng, Q Tian, X Zhao, L Bian, W Wang, Y Teng, R Ma, R Ahuja, W Luo, Z Zhang - Journal of Alloys and Compounds, 2025</p> <p>Abstract: Extraction of ^{90}Sr from groundwaters is of great significance in energy and ecological environment. Phosphate minerals have been proposed as a suitable matrix for the <i>in-situ</i> remediation of radionuclides from groundwaters by encouraging co-precipitation. However, the understanding of how Sr^{2+} precipitate into phosphate minerals affected by grain growth has not been fully resolved. In this work, the precipitation reaction of $\text{Sr}_5(\text{PO}_4)_3\text{OH}$ and SrHPO_4 were studied based on experiments and PHREEQC simulation. Some specific issues such as the precipitation reaction kinetics and the phase evolution during grain growth were discussed in detail, along with investigating the chemical stability of obtained precipitations before and after calcination. The results show that pH appears to be a prevailing factor with a recommended pH</p>

	<p>= 8 ~ 11 to obtain the stability domain of $\text{Sr}_5(\text{PO}_4)_3\text{OH}$ and SrHPO_4 to remove Sr^{2+} with a removal rate over 98 %. Interestingly, SrHPO_4 is more likely to preferentially nucleate at pH = 8 solution compared to $\text{Sr}_5(\text{PO}_4)_3\text{OH}$, and the poorly crystalline SrHPO_4 tends to disappear over time. TEM and SAXS results show the plate-like nanoparticles of SrHPO_4 are wrapped into the rod-like particles of $\text{Sr}_5(\text{PO}_4)_3\text{OH}$ during the grain growth, and the inner SrHPO_4 can react with $\text{Sr}_5(\text{PO}_4)_3\text{OH}$ to form $\text{Sr}_3(\text{PO}_4)_2$ at temperature over 600 °C. This observation is inconsistent with the previous grain growth result of poorly crystalline SrHPO_4, where it is believed to recrystallize into more stable $\text{Sr}_5(\text{PO}_4)_3\text{OH}$ crystals over time. Moreover, the Sr-O binding energy plays an important role in controlling the degradation of $\text{Sr}_5(\text{PO}_4)_3\text{OH}$, $\text{Sr}_3(\text{PO}_4)_2$, SrHPO_4 and $\beta\text{-Sr}_2\text{P}_2\text{O}_7$.</p> 
64.	<p>Secretome derived From Mesenchymal Stem cells cultured as monolayer show enhanced bone regeneration compared to secretome from 3D spheroid –clues from the proteome S Raik...S Kumar... N Kumar, S Bhattacharyya - Advanced Healthcare Materials, 2025</p> <p>Abstract: Repair and reconstruction of critical-sized bone defects present a significant challenge due to poor clinical outcomes of conventional bone repair strategies, such as autologous and allogenic bone grafts. The present study underscores the potential of human dental pulp stem cell-derived trophic factors to promote bone repair and regeneration, thus evading the risks associated with cell-based therapy. This study utilizes pre-osteoblast cells to evaluate the osteogenic potential of 2 Dimensional (2D) and 3 Dimensional (3D) secretome from monolayer and spheroid cultures of dental pulp stem cells (DPSCs), respectively. In-vitro results on pre-osteoblast cells (MC3T3-E1) treated with 2D and 3D secretome reveal lower mineralization and mRNA expression of osteogenic specific genes in 3D secretome in comparison to 2D secretome. Furthermore, 2D secretome shows better bone regeneration ability in rat models of calvarial bone defect compared to the 3D secretome. The proteomic profiles of 2D and 3D secretomes are also in concordance with these results and reveal key molecules governing bone regeneration potential. This data highlights the influence of culture conditions on the secretory pattern of mesenchymal stem cells and provides valuable insights for the development of a more effective secretome-based cell-free alternative for novel bone repair and regeneration.</p>
65.	<p>Shear dynamics around self-organized viscosity-stratified autocatalytic fronts in channel flows SN Maharana, M Mishra, L Rongy, A De Wit - Proceedings of the Royal Society A: Mathematical, Physical and Engineering Sciences, 2025</p> <p>Abstract: Vertical viscosity stratification in a channel flow driven by a longitudinal pressure gradient may induce shear instabilities that deform the interface into convective roll-ups. The initial position of the viscosity stratification, classically fixed in miscible non-reactive systems, crucially influences shear conditions in channel or pipe flows. Here, we investigate numerically convective shear dynamics when the position of the mixing zone evolves in time around a travelling autocatalytic reaction–diffusion front exhibiting self-organized viscosity changes. We analyse how the intersection between the travelling front position and the appropriate shear regions influences the onset time of the convective dynamics and the properties of the roll-ups. To do so, we consider a two-layered flow in a two-dimensional channel, where a more viscous solution of the autocatalytic species in the bottom layer invades a less viscous reactant solution perpendicularly to the direction of shear flow. Linear stability analysis (LSA) of the reaction–diffusion–convection equations suggests that, if the autocatalytic front is initially positioned at an intermediate vertical level, the flow can reach its most hydrodynamically unstable state. The</p>

	onset time of the convective dynamics obtained from nonlinear simulations matches the LSA predictions. Interestingly, nonlinear simulations highlight that the onset of roll-ups can be delayed while obtaining a maximum instability growth by tuning the speed of the autocatalytic chemical front.
66.	<p>S-Heterocyclic s-indacenodifluorene: Synthesis, properties and thermally tunable ambipolar field-effect mobility S Sahewal, S Ghosh, P Pradhan, PK Sharma, M Saifuddin, BK Patra, SP Senanayak, S Das - Chemistry - A European Journal, 2025</p> <p>Abstract: Design of semiconducting materials with facile control of charge transport and the nature of charge carriers is essential for realizing niche applications with organic electronics. Described herein are the synthesis, crystal structure, and analysis of the electronic properties of a four-stage redox amphoteric S-heterocyclic s-indacenodifluorene 6, including the study of its ambipolar charge carrier mobility (μ_h and μ_e) in organic field-effect transistor (OFET) devices. Despite being electron-rich, our investigation revealed reversible reduction potentials for 6 in the cyclic voltammetry, which is attributed to the recovery of locally aromatic thiophene and cyclopentadienyl anion units upon electron injection for the two antiaromatic S-heterocyclic as-indacene units in accordance with the Glidewell-Lloyd rule of aromaticity. In line with this, we observed an interesting thermal tunability of the nature of charge carriers from p-type to balanced ambipolar to n-type charge transport with reasonable semiconductor mobility in all regimes of transport. This behavior is correlated with the modification of the transport levels upon annealing of the semiconductor and possible increase in the extent of π-electron delocalization with increasing temperature. This proof-of-concept tunability of the nature of charge transport indicates the efficacy of our molecular design.</p> <div style="text-align: center;">  <ul style="list-style-type: none"> • First hetero-s-indacenodifluorene • Synthesis • Single-crystal • DFT calculations • (Anti)aromaticity • UV-vis-NIR absorption • Four-stage redox amphoterism • OFET device • Ambipolar charge-transport • Thermally-tuned p- to n-mobility </div>
67.	<p>Signature of interfacial water structure at the air–drug–polymer aqueous interface studied by sum frequency generation vibrational spectroscopy D Tomar, SK Sunnam, B Rana, I Sodhi, S Kaur, AT Sangamwar, SK Samal, KC Jena - The Journal of chemical physics, 2025</p> <p>Abstract: The selection of polymers suitable for the formulation of supersaturating drug-delivery systems is imperative to improve the solubility, thermodynamic stability, precipitation inhibition ability, and bioavailability of drugs <i>in vivo</i>. However, a detailed molecular-level understanding of finding the right drug–polymer combination in the aqueous medium is still ambiguous and often selected based on the trial procedure. Here, we have employed sum frequency generation vibrational spectroscopy (SFG-VS) to probe the impact of drug–polymer interactions on the interfacial water structure at the model biorelevant medium (BM) interface to extract better insights into the molecular system. We investigated two different polymers, Eudragit EPO (E-EPO) and polyvinylpyrrolidone K30 (P-K30), resulting in a considerable difference in the supersaturation limits of the atorvastatin calcium (ATC), the model drug molecule in the BM solution. The solubility study suggests an ~ 42 times enhancement in the solubility of ATC drug with the presence of E-EPO polymer and merely an ~ 2.6 times enhancement for polymer P-K30. Interestingly, SFG spectroscopic studies showed that E-EPO supports a substantial orientational ordering of the interfacial water molecules with the signature of strongly hydrogen (H)-bonded</p>

	<p>water molecules. An opposite trend is witnessed for the P-K30 polymer with less preferential ordering and weakly H-bonded water molecules at the air–BM interface. The microscopic insights from the SFG spectroscopy, in correlation with the observations on drug solubility, present a new potential approach for probing drug–polymer interactions. The implementation of SFG vibrational spectroscopy can be beneficial in selecting suitable polymers to adopt better strategies for bioavailability enhancement in drug formulation development.</p>
68.	<p>Strain-releasing hydrogenation of donor–acceptor Cyclopropanes and Cyclobutanes via electrochemical site selective carbonyl reduction N Banerjee, R Kumar, B Manna, P Banerjee - <i>The Journal of Organic Chemistry</i>, 2025</p> <p>Abstract: An acid or hydrogen gas-free electrochemical protocol is established for the hydrogenation of strained rings (cyclopropane and cyclobutane) at room temperature and atmospheric pressure. The mechanistic study revealed that the reaction was initiated via the reduction of the carbonyl group. The methodology is highly specific toward strained rings such as cyclopropane and cyclobutane, which exhibit broad functional group tolerance.</p> 
69.	<p>The grid interfaced pv-driven dual port solar system with improved depth of power extraction under solar irradiance disparity A Kumar, KR Sekhar, AS Kiran - <i>IEEE Transactions on Power Electronics</i>, 2025</p> <p>Abstract: This work introduces a dual solar port voltage-sharing grid-following inverter configuration with reduced operating DC bus potentials. The proposed configuration enhances energy extraction in medium and high-power applications by adeptly managing the solar irradiance disparities between input ports. Under disparities, an efficient solar power extraction method is proposed, utilizing a cascaded dual inverter configuration paired with a DC/DC converter to integrate the solar ports with the grid. In this configuration, the DC/DC converter works with the dual inverter for efficient energy extraction by maintaining the total DC bus voltage. However, the individual DC bus voltages vary according to the available solar power at each port. The designed control loop effectively handles the voltage asymmetry while maintaining the total DC bus voltage constant for seamless power injection to the grid. The voltage asymmetry across the individual inverters enhances the dual configuration's phase voltage levels, which helps improve the quality of the grid-injected current. Conversely, the voltage disparity influences the common mode voltages, but the magnitudes are under acceptable limits due to reduced operating DC bus potentials. The efficacy of the proposed configuration, along with its control methodology for handling solar irradiance disparity, is validated experimentally.</p>
70.	<p>Toxicological assessment of particulate and unregulated emissions from methanol and gasoline fueled reactivity controlled compression ignition engines NK Yadav, RK Maurya, V Chawla - <i>International Journal of Engine Research</i>, 2025</p> <p>Abstract: Reactivity-controlled compression ignition (RCCI) engines have emerged as a promising technology for achieving higher thermal efficiency while minimizing particulate (PM) and NOx emissions. However, concerns arise from the unregulated emissions of RCCI engines due to low temperature and premixed combustion. These unregulated species may condense on formed PM, potentially elevating the toxicity potential. This study investigates the toxicity potential of PM and unregulated emissions from RCCI engines employing gasoline and methanol</p>

	<p>as low-reactivity fuel and diesel as a high-reactivity fuel. In-vitro cytotoxicity tests with the BEAS-2B (human epithelial cell line) are conducted to characterize PM toxicity. A lung compartment model is used to estimate the particle risk, focusing on lung retention of PM particles emitted. Cancer risk potential is calculated for formaldehyde and acetaldehyde, constituents of unregulated emissions, to evaluate their impact on human health. Environmental risk assessment includes estimation of global warming potential, acidification potential, eutrophication potential, and ozone-forming potentials equivalents. Results indicate that with premixing ratio increases, unregulated emissions, cancer risk, cytotoxicity, and adverse environmental impacts increase. Methanol Diesel-RCCI engine particles exhibit lower lung retention than Gasoline Diesel-RCCI under all tested conditions. Methanol reduces cytotoxicity and particle inhalation toxicity at medium engine load. This study offers insights into the complex relationship between fuel, operating parameters, and the toxicity potential of emissions from RCCI engines.</p>
71.	<p>Unique determination of the damping coefficient in the wave equation using point source and receiver data M Vashisth - Proceedings-Mathematical Sciences, 2025</p> <p>Abstract: In this article, an inverse problem of determining the damping coefficient appearing in a wave equation is studied. We prove that the time-derivative perturbation of wave operator in three space dimension can be recovered uniquely from the data coming from a single coincident source-receiver pair. Since the problem under consideration is under-determined, so some extra assumption on the coefficient is required to prove the uniqueness.</p>
72.	<p>Unveiling an In-situ H₂O₂ production: Rechargeable Zinc-H₂O₂ battery powering 26 LEDs S Mehta, S Kaur, K Garg, M Singh, T C. Nagaiah - Angewandte Chemie, 2025</p> <p>Abstract: Looking towards ever-growing energy demand, the advancement in energy storage devices we have employed two bird-one stone approach viz.enabling 2e- oxygen electron reaction (ORR) to value added hydrogen peroxide (H₂O₂) product and its utilization in the energy storage devices using MnWO₄ catalyst, without any external H₂O₂ source. The designed catalyst exhibited a remarkable H₂O₂ production of 98% @ 0.37 V vs. RHE. The real time H₂O₂ production was monitored by in-situ electrochemical Raman and in-situ infrared spectroscopic measurements. The pivotal influence of electrolyte composition viz., local pH and the formation of carbonate species on H₂O₂ production was examined through micro-electrochemical studies using gold micro-electrode. Further, we assembled aqueous Zn-H₂O₂ battery which exhibited remarkable cycle life of 140 hours and energy efficiency of 43%. The Zn-H₂O₂ battery attained capacity of 25 mAh cm⁻² at 3 mA cm⁻² with ≥ 90 % of cycle efficiency and stability for more than 140 hours. and exhibited a stable OCV of 3.2 V for more than 200 hours with a promising power density of 10.5 mW cm⁻². As a proof of concept, we have demonstrated Zn-H₂O₂ batteries by powering 26 LEDs for more than 180 hours (7 days) without fading in the illumination of LEDs.</p>

[Viscoelasticity-contrast driven electrohydrodynamic behaviour of a droplet-suspended-in-a-confined-liquid configuration](#)

P Gupta, P Dhar, D Samanta - Journal of Non-Newtonian Fluid Mechanics, 2025

73.

Abstract: We present an approximate analytical model (without compromise on the physics) of the electrohydrodynamics (EHD) of a confined leaky dielectric, non-Newtonian viscoelastic droplet suspended in a surrounding medium of similar characteristics. The analysis considers the Stokes flow regime through a small deformation formulation. The viscoelastic behaviour is realized by coupling the Cauchy momentum equation with the upper convected Maxwell (UCM) model. Since the study is limited to low electric field intensities, the governing Weissenberg number ($Wi \leq 1$). We consider various combinations of the droplet and the surrounding, viz. NN-N, N-NN, and NN-NN cases. A thorough comparison with the N-N case is conducted. Here, ‘N’ represents Newtonian and ‘NN’ represents non-Newtonian. The solution put forward is validated with experimental observations in literature and works successfully in the regime of low electric field strength. We show that, for an unconfined domain, the deformation is maximum for the N-N case and least for the N-NN case, thus establishing the role of viscoelasticity-contrast. For the confined domain, we have also observed shape reversal in N-NN and NN-NN cases at higher confinement (α) and lower electro-rheological parameter (δ). For NN-N, the deformation is greater compared to the N-N case beyond a critical α . We also report the streamline patterns within the droplet and in the surrounding medium for various cases and for different confinement. The findings reveal shape reversal phenomena in confined viscoelastic cases, and provide insights into the EHD with fluidic confinement, offering potential avenues for the design and functionality of microfluidic devices.

Disclaimer: This publication digest may not contain all the papers published. Library has compiled the publication data as per the alerts received from Scopus and Google Scholar for the affiliation “Indian Institute of Technology Ropar” for the month of April, 2025. The author(s) are requested to share their missing paper(s) details if any, for the inclusion in the next publication digest.